On the computation of the Baer-Nunziato model

Fabien Crouzet, Frédéric Daude, Pascal Galon, Philippe Helluy, Jean-Marc Hérard, Yujie Liu

On the Computation of the Baer-Nunziato Model

Fabien Crouzet, Frédéric Daude*
EDF, R&D, 1 avenue du Général de Gaulle, 92141, Clamart, France

Pascal Galon†
CEA Saclay, 91191, Gif sur Yvette, France

Philippe Helluy‡
IRMA, 7 rue Descartes, Université de Strasbourg, 67084, Strasbourg, France

Jean-Marc Hérard§
EDF, R&D, 6 quai Watier, 78400, Chatou, France.

Yujie Liu ¶
EDF, R&D, 1 avenue du Général de Gaulle, 92141, Clamart, France

This paper is devoted to the computation of the Baer-Nunziato model, and more precisely to the verification of a few schemes, while using analytic solutions of the one-dimensional Riemann problem. Since classical perfect gas EOS may imply specific behaviours, we wish to investigate any kind of EOS, and thus we focus on and verify capabilities and drawbacks of simple enough solvers such as the Rusanov scheme. For so-called first-order (respectively second-order) Finite-Volume schemes, we check that a $h^{1/2}$ (resp. $h^{2/3}$) rate of convergence is retrieved. Actually, the fractional step approach is also shown to be more stable than the single-step approach.

Introduction

The numerical prediction of water-hammer flows may be achieved while retaining the homogeneous approach or the two-fluid approach. The latter has been investigated in the framework of the Wahaloads project (see[35]). Another possibility suggests not to get rid of pressure-velocity-temperature relaxation time scales, which means that one needs to recover the governing equations for seven main variables: the statistical void fraction, together with the mean velocity, the mean pressure and the mean temperature within each phase (the liquid phase and the vapour phase). A rather large frame of two-fluid models can be found in references[4,6,24,25,30] among others, when restricting to gas-particle flows, and otherwise in references[8,13,14,19,23] for gas-liquid or water-vapour flows. Among these models, the Baer-Nunziato model has a significant field of applications, and focus will be given here on this model.

Actually, the computation of Baer-Nunziato type models is indeed a real challenge, due to the fact that the convective subset of equations involves two (or three, depending on the form of the interface velocity) distinct contact waves, which are roughly equal to mean phase field velocities (see the next section below). Hence, based on classical results of the literature dealing with Euler equations (see[10–12] among others), we

*Research Engineer, EDF R&D AMA, and: LaMSID, UMR EDF/CNRS/CEA 2832, 1 avenue du Général de Gaulle, 92141, Clamart, France.

†Research Engineer, CEA, Saclay, France, and: LaMSID, UMR EDF/CNRS/CEA 2832, 1 avenue du Général de Gaulle, 92141, Clamart, France.

‡Professor, IRMA, 7 rue Descartes, Université de Strasbourg, 67084, Strasbourg, France.

§Senior engineer, EDF R&D, MFEE, 6 quai Watier, 78400, Chatou, France.

¶PhD student, EDF, R&D, AMA and: LaMSID, UMR EDF/CNRS/CEA 2832, 1 avenue du Général de Gaulle, 92141, Clamart, France, and: LATP, UMR CNRS 7353, 39 rue Joliot Curie, 13453, Marseille, France.

may expect that the rate of convergence of Finite Volume algorithms relying on Riemann interface solvers would be low, typically varying as $h^{1/2}$ for so-called first-order Finite-Volume schemes. Moreover, intermediate states arising between the two contact discontinuities are difficult to predict, since the Mach number $(U_v - U_l)/c_l$ is small compared with 1 in almost all real-life situations, which results in the fact that the two contact waves are close to one another, and thus slow down the increase of accuracy. These expectations were actually confirmed quite recently in reference[23] in the fluid case, and in[15,16,20] when computing approximate solutions of the two-fluid model in a porous framework.

Another point which seems worth being recalled, and which precisely emerges from the latter porous context, is that some naive schemes (such as Rusanov scheme) may fail at providing approximate solutions that converge towards the *correct* weak solutions, when focusing on two-fluid models such as Baer-Nunziato model. Most of the time, this may be simply checked by inserting suitable "well-balanced" data (in a sense to be defined) in the initial conditions of the one-dimensional Riemann problem; actually, this will be discussed in detail in the sequel (see section V).

Last but not least, almost all Riemann solvers proposed up to now in the literature rely on EOS which have a very particular form, since these rely on the use of either perfect gas EOS (PG), or alternatively stiffened gas EOS (SG). A straightforward consequence is that this may hide deficiencies which are tightly linked with the *non-linear* expressions arising in thermodynamical functions.

These remarks have motivated the following investigation, which has a multi-fold purpose:

- We wish to investigate Rusanov scheme which may not only handle perfect gas (or stiffened gas) EOS, but also -almost- any kind of relevant EOS, without introducing a huge increase of CPU time per cell per time step, and we intend to give special focus on numerical rates of convergence, whenever a first or second-order version is used;
- We aim at examining whether this simple enough Riemann solver is well-balanced with respect to the void fraction coupling wave; otherwise, we must check whether the solver forbids convergence towards correct solutions -or not- when the mesh is refined;
- Eventually, we will compare this basic solver with another scheme relying on the fractional step strategy.

The present paper is organised as follows. We first recall the basic set of governing equations of the Baer-Nunziato model, together with its main properties. Next we define some basic solutions of the one-dimensional Riemann problem associated with the latter model, while focusing on void fraction waves, whatever the EOS of liquid and vapour are. The following section details the basic Rusanov Finite Volume solver that is used to compute approximate solutions, and some of its associated properties; a simple alternative scheme will also be presented in the sequel. The last section will be devoted to numerical results that will allow an estimation of rates of convergence. Eventually some conclusions will be drawn.

I. The Baer-Nunziato model

If indexes l, v refer to the liquid and vapour phases, we may define the statistical void fractions of vapour and liquid α_v and α_l, which comply with:

$$\alpha_l + \alpha_v = 1 \ ;$$

Besides, $P_{l,v}$, $U_{l,v}$ and $\rho_{l,v}$ respectively denote the mean pressures, mean velocities and mean densities of the two phases for the liquid and vapour phases. Assuming that equations of state are given, and that functions $e_\phi(P_\phi, \rho_\phi)$ are known, the total energy reads:

$$E_\phi = \rho_\phi e_\phi(P_\phi, \rho_\phi) + \rho_\phi \frac{U_\phi^2}{2}, \qquad \phi = v, l \tag{1}$$

Partial masses will be noted $m_\phi = \alpha_\phi \rho_\phi$. We define W as follows:

$$W = (\alpha_l, \alpha_l\rho_l, \alpha_l\rho_l U_l, \alpha_l E_l, \alpha_v\rho_v, \alpha_v\rho_v U_v, \alpha_v E_v)$$

Hence, when focusing on liquid flows containing a small amount of vapour bubbles, the Baer-Nunziato model may be written as follows:

$$\begin{cases} \partial_t(\alpha_l) + U_v \partial_x(\alpha_l) = S_{1,l} \\ \partial_t(\alpha_l\rho_l) + \partial_x(\alpha_l\rho_l U_l) = S_{2,l} \\ \partial_t(\alpha_l\rho_l U_l) + \partial_x\left(\alpha_l\rho_l U_l^2 + \alpha_l P_l\right) - P_l\partial_x(\alpha_l) = S_{3,l} \\ \partial_t(\alpha_l E_l) + \partial_x(\alpha_l U_l(E_l + P_l)) + P_l\partial_t(\alpha_l) = S_{4,l} \\ \partial_t(\alpha_v\rho_v) + \partial_x(\alpha_v\rho_v U_v) = -S_{2,l} \\ \partial_t(\alpha_v\rho_v U_v) + \partial_x\left(\alpha_v\rho_v U_v^2 + \alpha_v P_v\right) - P_l\partial_x(\alpha_v) = -S_{3,l} \\ \partial_t(\alpha_v E_v) + \partial_x(\alpha_v U_v(E_v + P_v)) + P_l\partial_t(\alpha_v) = -S_{4,l} \end{cases} \tag{2}$$

where right-hand side terms $S_{k,l}(W)$ represent the source terms (for $k = 2, 3, 4$) that account for mass transfer, momentum and energy transfer through the interface between the two phases. The exact expressions of terms $S_{1,l}$ can be found in[4,6,9,14,18,23–25] . The celerity of acoustic waves in the pure liquid (respectively vapour) phase is noted c_l (resp. c_v), and the phase entropy s_ϕ complies with:

$$(c_\phi)^2 = -\partial_{\rho_\phi}(s_\phi)/\partial_{P_\phi}(s_\phi) \tag{3}$$

A. Main properties of Baer-Nunziato model

We recall the main properties of system (2). Most of them are classical and can be found in[2,8,13] , together with proofs, comments and details.

- **Property 1** *(hyperbolicity):*
  The set of equations (2) is hyperbolic. It admits seven real eigenvalues:

  $$\lambda_{1,2} = U_v, \quad \lambda_3 = U_v - c_v, \quad \lambda_4 = U_v + c_v, \quad \lambda_5 = U_l, \quad \lambda_6 = U_l - c_l, \quad \lambda_7 = U_l + c_l$$

  and associated righteigenvectors span the whole space $\mathcal{R}^7$, unless $|U_l - U_v|/c_l = 1$;

- **Property 2** *(entropy inequality) :*
  Define the entropy $\eta(W) = m_l s_l + m_v s_v$ and the entropy flux $f_\eta(W) = m_l s_l U_l + m_v s_v U_v$; then smooth solutions W of (2) are such that:

  $$0 \leq \partial_t(\eta(W)) + \partial_x(f_\eta(W)). \tag{4}$$

- **Property 3** *(structure of fields, Riemann invariants through LD waves and jump conditions) :*

  Fields associated with eigenvalues $\lambda_{1,2,5}$ are linearly degenerate (LD). Other fields are genuinely non linear (GNL). The five Riemann invariants of the $1-2$ LD field associated with the void fraction coupling wave are the following:

  $$\begin{array}{lll} I^1_{1-2}(W) = U_v; & ; I^2_{1-2}(W) = s_l; & \\ I^3_{1-2}(W) = m_l(U_l - U_v); & ; I^4_{1-2}(W) = \alpha_l P_l + \alpha_v P_v + m_l(U_v - U_l)^2; & \\ I^5_{1-2}(W) = e_l + P_l/\rho_l + (U_v - U_l)^2/2; & & \end{array} \tag{5}$$

  The structure of the 5 LD wave is classical, since:

  $$\begin{array}{lll} I^1_5(W) = U_l; & ; I^2_5(W) = P_l; & \\ I^3_5(W) = \alpha_l; & ; I^4_5(W) = P_v; & \\ I^5_5(W) = U_v; & ; I^6_5(W) = \rho_v & \end{array} \tag{6}$$

  Within each isolated field associated with $\lambda_k = 3, 4, 6, 7$, unique jump conditions hold. If σ denotes the speed of the shock wave, and L, R the left-right states on each side of this travelling discontinuity,

these are:

$$\begin{array}{l} [\alpha_v]_l^r = 0; \\ -\sigma[\rho_\phi]_l^r + [\rho_\phi U_\phi]_l^r = 0; \\ -\sigma[\rho_\phi U_\phi]_l^r + [\rho_\phi U_\phi^2 + P_\phi]_l^r = 0; \\ -\sigma[E_\phi]_l^r + [U_\phi(E_\phi + P_\phi)]_l^r = 0, \end{array} \tag{7}$$

Thus, shock relations are exactly single-phase shock relations, field by field. Moreover, Riemann invariants of the latter $3, 4$ waves (and $6, 7$ waves respectively) coincide with those of the pure single vapour (respectively liquid) phase.

Remark 1:
A crucial feature of the Baer-Nunziato model is that non-conservative products are only active through the $1-2$-wave which is LD; hence jump conditions are unique, and this implies that it makes sense computing shock solutions (and these may be checked).

B. Specific solutions of the one-dimensional Riemann problem

This section is devoted to the construction of simple analytic solutions of the one-dimensional Riemann problem associated with Baer-Nunziato model, which correspond to pure void fraction contact waves. For that purpose, we start with a given left state W_L, and also prescribe two values for $(\alpha_l)_R$ and $(\rho_v)_R$ on the right side, and we assume that the solution of the Riemann problem contains only one -double- contact wave associated with $\lambda_{1,2}$. Hence we wonder whether we can find $(P_v, P_l, U_v, U_l, \rho_l)_R$ such that :

$$I_{1-2}^k(W_R) = I_{1-2}^k(W_L) \qquad for: \quad k = 1 - 5. \tag{8}$$

We get at once that

$$(U_v)_R = (U_v)_L, \tag{9}$$

and also, setting $X = (\rho_l)_R$ and $Q_L = (m_l(U_l - U_v))_L$:

$$(U_l)_R = (U_v)_L + Q_L/((\alpha_l)_R X). \tag{10}$$

Eventually, setting $Y = (P_l)_R$, we can deduce $(P_v)_R$ from:

$$(1 - (\alpha_l)_R)(P_v)_R = I_{1-2}^4(W_L) - (\alpha_l)_R Y - (Q_L)^2/((\alpha_l)_R X) \tag{11}$$

On the whole, introducing $H_L = e_l((P_l)_L, (\rho_l)_L) + (P_l)_L/(\rho_l)_L + ((U_l - U_v)_L)^2/2$, and also $S_L = s_l((\rho_l)_L, (P_l)_L)$, we need to find $(X > 0, Y)$ solution of the coupled problem:

$$\begin{array}{l} s_l(X, Y) = S_L; \\ e_l(X, Y) + Y/X + (Q_L)^2/(2(\alpha_l)_R^2 X^2) = H_L. \end{array} \tag{12}$$

We may define the solution $Y = \Phi(X)$ of the first equation in (12), and check that $\Phi'(X) > 0$, whatever the EOS of the liquid phase is. Thus we need to find X solution of:

$$f(X) \stackrel{def}{=} e_l(X, \Phi(X)) + \Phi(X)/X + A^2/X^2 - H_L = 0. \tag{13}$$

where we note $A^2 = (Q_L)^2/(2(\alpha_l)_R^2)$. Then we get:

Proposition 1:
Define X_0 solution of $X^2\Phi'(X) = 2A^2$; then, system (12) admits at least one solution if:

$$f(X_0) < 0.$$

The proof is left to the reader.

Remark 2:
For a practical implementation, we may for instance compute X_0 for a stiffened gas EOS for the liquid phase, setting:

$$e_l(\rho_l, P_l) = (P_l + \gamma_l P_\infty)/((\gamma_l - 1)\rho_l)$$

with $\gamma_l > 1$. In that case, we get a unique value:

$$X_0 = (2A^2/(\gamma_l S_L))^{1/(\gamma_l+1)}$$

and it may be checked that equation (13) *admits two distinct solutions X_1, X_2 if $f(X_0) < 0$. These may be used to complete the right initial condition W_R, defining $(P_l)_R = \Phi(X)$, $(U_v)_R = (U_v)_L$ and $(P_v, U_l)_R$ from* (11), (10) *; the value of $(\rho_v)_R$ must be prescribed independently. In the sequel, these specific initial conditions (W_L, W_R) will be refered to as "well-balanced initial data for the void fraction wave (VFW)". We also emphasize that, for given non-zero value of Q_L, the contribution A^2/X_0^2 varies as $(Q_L/(\alpha_l)_R)^{2(\gamma_l-1)/(\gamma_l+1)}$, and thus tends to $+\infty$ when $(\alpha_l)_R$ vanishes; this means that for $(\alpha_l)_R$ small enough, equation* (13) *will not admit any solution X.*

Remark 3:
By the way we quote at once that the counterpart of the construction of the approximate Godunov solver proposed in[33] *, where the EOS of the liquid phase is a perfect gas EOS, becomes much more difficult (and CPU time consuming) in the case of an arbitrary liquid EOS.*

Remark 4:
Following the basic ideas of[27] *, we note that the above construction of "well-balanced initial data for the VFW" might be used to construct a modified version of Rusanov scheme, using a Euler-Lagrange formulation of the scheme (see*[7, 15] *also).*

II. Basic algorithm

The overall algorithm is grounded on the use of the fractional step method. An "evolution" step computes approximations of solutions of the convective effects, while the second step enables to account for source terms.

- *Step 1 : with given initial values W^n, compute approximate solutions of the hyperbolic homogeneous system:*

$$\left\{\begin{array}{l} \partial_t(\alpha_l) + U_v \partial_x(\alpha_l) = 0 \\ \partial_t(\alpha_l\rho_l) + \partial_x(\alpha_l\rho_l U_l) = 0 \\ \partial_t(\alpha_l\rho_l U_l) + \partial_x\left(\alpha_l\rho_l U_l^2 + \alpha_l P_l\right) - P_l\partial_x(\alpha_l) = 0 \\ \partial_t(\alpha_l E_l) + \partial_x(\alpha_l U_l(E_l + P_l)) + P_l\partial_t(\alpha_l) = 0 \\ \partial_t(\alpha_v\rho_v) + \partial_x(\alpha_v\rho_v U_v) = 0 \\ \partial_t(\alpha_v\rho_v U_v) + \partial_x\left(\alpha_v\rho_v U_v^2 + \alpha_v P_v\right) - P_l\partial_x(\alpha_v) = 0 \\ \partial_t(\alpha_v E_v) + \partial_x(\alpha_v U_v(E_v + P_v)) + P_l\partial_t(\alpha_v) = 0 \end{array}\right. \tag{14}$$

  through the time interval $[t^n, t^n + \Delta t]$; hence, a set of approximations $\tilde{W}$ is obtained; then:

- *Step 2: with given initial values $\tilde{W}$, compute approximations of the set of ODEs:*

$$\left\{\begin{array}{l} \partial_t(\alpha_l) = S_{1,l} \\ \partial_t(\alpha_l\rho_l) = S_{2,l} \\ \partial_t(\alpha_l\rho_l U_l) = S_{3,l} \\ \partial_t(\alpha_l E_l) + P_I\partial_t(\alpha_l) = S_{4,l} \\ \partial_t(\alpha_v\rho_v + \alpha_l\rho_l) = 0 \\ \partial_t(\alpha_v\rho_v U_v + \alpha_l\rho_l U_l) = 0 \\ \partial_t(\alpha_v E_v + \alpha_l E_l) = 0 \end{array}\right. \tag{15}$$

  through the time interval $[\tilde{t}, \tilde{t} + \Delta t]$, which gives approximations of W at time t^{n+1}.

We focus in this paper on the computation of the evolution step (14)**,** and the reader is refered to[9, 13, 22, 23] for details concerning the treatment of source terms in (15).

III. An extension of Rusanov scheme for Baer-Nunziato model

Before going further on, we recall that system (14) may be rewritten as follows:

$$\partial_t (W) + \partial_x (\mathcal{F}(W)) + \mathcal{H}(W)\partial_x (\alpha_l) = 0 \tag{16}$$

where:

$$\mathcal{H}(W) = (U_v, 0, -P_l, -P_l U_v, 0, P_l, P_l U_v)$$

We present now a classical extension of the conservative Rusanov scheme[31] in order to obtain approximate solutions of system (16).

We denote Δt the time step and h_i the size of cell Ω_i. We compute W_i^{n+1} in terms of neighbouring cells W_k^n (for $k = i-1, i, i+1$) using the following three-point scheme:

$$h_i(W_i^{n+1} - W_i^n) + \Delta t(f_{i+1/2}^{Rusanov}(W_i^n, W_{i+1}^n) - f_{i-1/2}^{Rusanov}(W_{i-1}^n, W_i^n)) + \Delta t \mathcal{T}_i^n = 0 \tag{17}$$

where the numerical flux through the interface $(i+1/2)$ separating cells i and $i+1$ is:

$$f_{i+1/2}^{Rusanov}(W_i^n, W_{i+1}^n) = ((\mathcal{F}(W_i^n) + \mathcal{F}(W_{i+1}^n)) - r_{i+1/2}(W_{i+1}^n - W_i^n))/2 \tag{18}$$

The scalar $r_{i+1/2}$ is equal to $max(R_i^n, R_{i+1}^n)$, where R_k^n is the spectral radius of the whole convection matrix associated with (16) and estimated at W_k^n, for $k = i, i+1$:

$$R_k^n = max(|(U_l)_k^n| + (c_l)_k^n, |(U_v)_k^n| + (c_v)_k^n)$$

The term $\mathcal{T}_i^n$ is:

$$\mathcal{T}_i^n = \mathcal{H}(W_i^n)\left((\overline{\alpha}_l)_{i+1/2}^n - (\overline{\alpha}_l)_{i-1/2}^n\right) \tag{19}$$

while setting: $\overline{\phi}_{k+1/2}^n = (\phi_k^n + \phi_{k+1}^n)/2$. This scheme, which will refered to as **SR1** in the sequel, enjoys the following property:

Property 4:
Scheme (17), (18), (19) *preserves positive values of partial masses* m_ϕ *and void fractions* α_ϕ, *for* $\phi = l, v$, *provided that the following CFL-like condition holds on the time step* Δt*:*

$$\Delta t(r_{i-1/2} + r_{i+1/2}) < 2h_i \tag{20}$$

See[23] for proof.

Remark 5:
The scheme (17), (18), (19) *does not maintain "well-balanced initial data for the VFW" on any mesh. This means that if the initial condition* W_j^n *is such that for* $k = 1$ *to* 5*:*

$$I_{1,2}^k(W_j^n) = \mathcal{I}_0^k$$

for all j, *the updated values* W_j^{n+1} *will not comply with :* $I_{1,2}^k(W_j^{n+1}) = \mathcal{I}_0^k$ *for all* j. *Thus we will examine later on whether the scheme converges towards the correct solution when the mesh is refined. We emphasize here that available solvers in the literature do not preserve "well-balanced initial data for the VFW" in the above defined sense.*

We present now a fractional step method in order to get other approximations of solutions of the homogeneous subset (14).

IV. A fractional step method to compute Baer-Nunziato model

The fractional step method may be useful in order to get approximations of solutions of homogeneous hyperbolic systems of conservation laws. This idea has been successfully used by Baraille and Leroux (see[5]) in order to obtain approximate solutions of Euler equations, and several authors have been using the same strategy for various purposes. Among these, we note that hybrid explicit/implicit schemes may be constructed that way.

The basic idea here is to construct a fractional-step scheme that would comply with the following requirements:

- (i) The scheme should preserve hyperbolicity within each step;
- (ii) The scheme should preserve the pseudo-conservative form of the whole set of equations;
- (iii) The Riemann problem associated with each substep should be easier to solve.

Moreover, the fractional step method should be such that it might handle Baer-Nunziato type models such as those introduced in reference[21] .

The particular scheme we examine here is the following. Starting with an initial condition W_i^n, we compute first some approximation of solutions of:

$$\begin{cases} \partial_t(\alpha_l) + U_v \partial_x(\alpha_l) = 0 \\ \partial_t(\alpha_l \rho_l) = 0 \\ \partial_t(\alpha_l \rho_l U_l) = 0 \\ \partial_t(\alpha_l E_l) + P_l \partial_t(\alpha_l) = 0 \\ \partial_t(\alpha_v \rho_v) = 0 \\ \partial_t(\alpha_v \rho_v U_v) = 0 \\ \partial_t(\alpha_v E_v) + P_l \partial_t(\alpha_v) = 0 \end{cases} \tag{21}$$

and then use final values $\hat{W}_j$ as an initial condition for the computation of approximate solutions of :

$$\begin{cases} \partial_t(\alpha_l) = 0 \\ \partial_t(\alpha_l \rho_l) + \partial_x(\alpha_l \rho_l U_l) = 0 \\ \partial_t(\alpha_l \rho_l U_l) + \partial_x\left(\alpha_l \rho_l U_l^2 + \alpha_l P_l\right) - P_l \partial_x(\alpha_l) = 0 \\ \partial_t(\alpha_l E_l) + \partial_x(\alpha_l U_l (E_l + P_l)) = 0 \\ \partial_t(\alpha_v \rho_v) + \partial_x(\alpha_v \rho_v U_v) = 0 \\ \partial_t(\alpha_v \rho_v U_v) + \partial_x\left(\alpha_v \rho_v U_v^2 + \alpha_v P_v\right) - P_l \partial_x(\alpha_v) = 0 \\ \partial_t(\alpha_v E_v) + \partial_x(\alpha_v U_v (E_v + P_v)) = 0 \end{cases} \tag{22}$$

Obviously, criterion (ii) is fullfilled. Moreover, the previous fractional step method has the following properties:

Proposition 2:

- (i) *System* (21) *is hyperbolic. It admits seven real eigenvalues:*

$$\lambda_1 = U_v \qquad \lambda_{2-7} = 0$$

and its right eigenvectors span $\mathcal{R}^7$*. All fields are linearly degenerated. The six Riemann invariants through the* 1*-field are:* $\{m_l, m_v, U_l, U_v, s_l, m_l e_l + m_v e_v\}$ *. Besides,* α_l *is the only Riemann invariant of the* $2-7$*-wave.*

- (ii) *System* (22) *is hyperbolic. It admits seven real eigenvalues:*

$$\begin{aligned}
&\lambda_1 = 0 \\
&\lambda_2 = U_v, \quad \lambda_3 = U_v - c_v, \quad \lambda_4 = U_v + c_v, \\
&\lambda_5 = U_l, \quad \lambda_6 = U_l - c_l, \quad \lambda_7 = U_l + c_l
\end{aligned} \tag{23}$$

and associated right eigenvectors span $\mathcal{R}^7$*, unless:* $|U_l| = c_l$*, or:* $|U_v| = c_v$*. The* $1, 2, 5$*-fields are LD and other fields are genuinely non linear. Riemann invariants of the steady* 1*-wave are:* $\{m_l U_l, m_v U_v, H_l, H_v, \Sigma_{k=l,v}(m_k U_k^2 + \alpha_k P_k), s_l\}$*, setting as usual* $H_k = e_k + P_k/\rho_k + U_k^2/2$*. The solution of the Riemann problem associated with the liquid phase is the same as the one associated with one-dimensional compressible Euler equations in a variable cross section* $A(x) = \alpha_l(x)$*.*

We refer to[28] which examines in detail the solution of the Riemann problem associated with (21) and (22), and also to[32,34] and associated references for the investigation of compressible Euler equations in a variable cross-section duct. Though it is not discussed in this paper, one additional advantage of this fractional step method is that it enables to tackle systems such as the one arising in[21] .

In order to compute approximate solutions of system (21), we use a Rusanov flux formulation applied to:

$$\partial_t(\alpha_l) + U_v \partial_x(\alpha_l) = 0 \tag{24}$$

while keeping partial masses and velocities frozen:

$$(\hat{m}_k)_i = (m_k)_i^n \qquad (\hat{U}_k)_i = (U_k)_i^n \qquad \textit{for:} \quad k = l, v$$

and setting :

$$\begin{aligned}
&(\hat{\alpha}_l \hat{E}_l + \hat{\alpha}_v \hat{E}_v)_i = (\alpha_l E_l + \alpha_v E_v)_i^n \\
&(\hat{\alpha}_v \hat{E}_v)_i - (\alpha_v E_v)_i^n - (P_l)_i^n (\hat{\alpha}_{li} - (\alpha_l)_i^n) = 0
\end{aligned} \tag{25}$$

This substep provides an estimate value $\hat{W}_j$ within each cell j that is used to initialize the second substep corresponding with (22).

We also use the generic Rusanov formulation detailed above to compute approximations of solutions of the second step (22) (see[28]). Positive values of statistical void fractions $\alpha_{l,v}$ and partial masses $m_{l,v}$ are guaranteed by the scheme if the time step is constrained by (20).

Remark 6:
Following[15,27] *, we know that the computation of approximate solutions of* (22) *should be done with great care, since wrong solutions may be captured, due to the occurence of the steady wave. This will be examined later on while focusing on* L^1 *norms of the error. Moreover, the solution of the one-dimensional Riemann problem associated with variables of the vapour phase cannot be obtained at once, unless the term* $P_l \partial_x(\alpha_l)$ *in the governing equation of the momentum* $m_v U_v$ *is frozen.*

V. Numerical results

As it has been mentionned before, we will give emphasis here on the numerical capabilities of schemes and more precisely on numerical rates of convergence. The first two test cases correspond to classical Riemann problems of the literature. The last test case aims at providing some deeper insight on pure void fraction waves.

A. Test case 1

This Riemann problem was introduced in[33] , and it involves two perfect gas EOS for the two phases. The exact solution of the Riemann problem is recalled below by providing values of intermediate states (see table 1). Figure 1 shows the evolution of the L^1 norm of the error as a function of the mesh size, when the time step complies with the constraint $CFL = 1/2$. The coarser and finer meshes contain 100 and 10^5 cells respectively. Figure 2 shows the approximate solutions for $\alpha_l, \rho_l, \rho_v, U_l, U_v, P_l, P_v$ that have been obtained

with 200 and 500 cells, either using the "first-order" Rusanov scheme **SR1**, or a "second-order" extension of the Rusanov scheme **SR1-ORDER2**. The second-order scheme is grounded on a minmod reconstruction of the symmetrizing variable $Z^t = (\alpha_l, U_l, U_v, P_l, P_v, s_l, s_v)$ within each cell i, setting:

$$Z_i(x, t^n) = Z_i^n + (x - x_i)(\nabla Z)_i^n$$

where:

$$h_i(\nabla Z)_i^n = sign(Z_{i+1}^n - Z_i^n)\dot{(}min(|Z_{i+1}^n - Z_i^n|, |Z_{i-1}^n - Z_i^n|)) \quad \text{if:} \quad (Z_{i+1}^n - Z_i^n)(Z_i^n - Z_{i-1}^n) > 0$$

and $(\nabla Z)_i^n = 0$ otherwise. A second-order Runge-Kutta time scheme is used for time integration. Obviously, we retrieve the expected rates of convergence : 1/2 and 2/3 for the first-order and second-order schemes respectively. These results are in agreement with those of[10,11,15] . We recall that the slow rate of convergence is enforced by the contact discontinuities.

Perfect gas EOS with $\gamma_l = \gamma_v = 7/5$

	Left initial condition	Region 1	Region 0	Region 2	Right initial condition
α_v	0.8	0.8	0.8	0.3	0.3
ρ_v	1.0	0.9436	0.9436	1.0591	1.0
u_v	0.0	0.0684	0.0684	0.0684	0.0
p_v	1.0	0.9219	0.9219	1.0837	1.0
ρ_l	0.2	0.3266	0.6980	0.9058	1.0
u_l	0.0	-0.7683	-0.7683	-0.1159	0.0
p_l	0.3	0.6045	0.6045	0.8707	1.0

Table 1. Initial condition and intermediate states arising in the solution of a test case by Schwendeman-Wahle-Kapila (see reference[33] page 499).

B. Test case 2

This test case is taken from[36] (pages 3854-3585). A perfect gas EOS is used for the vapour phase, while a stiffened gas EOS is retained for the liquid phase (see table 2). Regular meshes have been used , which

Perfect gas EOS for vapour ($\gamma_v = 1.35$) and stiffened gas EOS for liquid $\gamma_l = 3, (p_l)_\infty = 3400$

	Region L	Region 1	Region 0	Region 2	Region R
α_v	0.8	0.8	0.1	0.1	0.1
ρ_v	2.0	2.1093	1.6733	1.8554	1.0
u_v	0.0	-0.0761	0.7912	0.7912	0.0
p_v	3.0	3.2235	2.3580	2.3580	1.0
ρ_l	1900.0	2040.1092	1821.4053	1821.4053	1950.0
u_l	0.0	-0.1716	-0.1716	-0.1716	0.0
p_l	10.0	824.4354	185.6560	185.6560	1000.0

Table 2. Initial conditions and intermediate states for test case 2 proposed by Tokareva and Toro (see reference[36]).

contain 200, 500, 10^3, 5×10^3, 10^4, 5×10^4 cells. The CFL number is still 1/2, and the computation is stopped at $t = 0.15$. While focusing on the first-order Rusanov and fractional-step schemes **SR1** and **PFRAC32**, we plot the L^1 norm of the error in figure 3. We retrieve the expected $h^{1/2}$ rate of convergence for all variables. The exact solution together with approximate solutions of variables $\alpha_v, \rho_k, u_k, p_k,\ k = l, v$

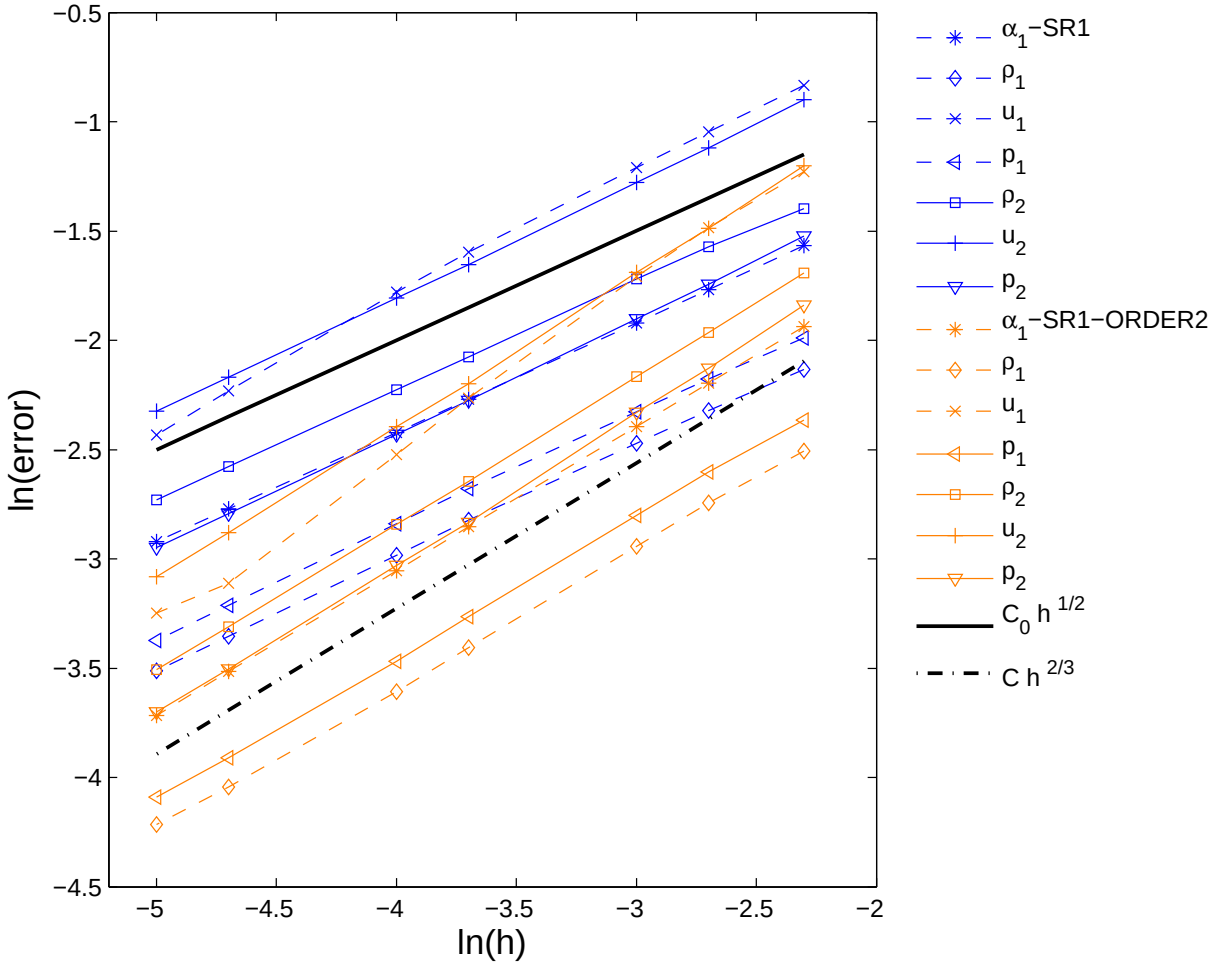

Figure 1. Convergence curves for $\alpha_1, \rho_k, u_k, p_k,\ k = 1, 2$ for test case 1 by Schwendeman-Wahle-Kapila. Results have been obtained with first-order and second-order SR1 and SR1-ORDER2 schemes , setting: $CFL = 1/2,\ t = 0.2$. The black line is a reference $C_o h^{1/2}$.

obtained with 500 and 5000 cells are displayed in figure 4. We note that intermediate states are rather well captured by both schemes on these rather coarse meshes.

The next figure 5 shows the convergence rates for first-order and second-order schemes **SR1** and **SR1-ORDER2**. Moreover, the exact solution together with approximate solutions of variables $\alpha_v, \rho_k, u_k, p_k,\ k = l, v$ obtained while using 200 and 500 cells, are displayed in figure 6. Once more, a $h^{2/3}$ rate of convergence is observed for the second-order scheme, for all components of the state variable. No oscillations can be noticed around shock waves and contact discontiniuties for the second-order scheme.

C. Test case 3

This last test case is actually much more difficult. It simply corresponds to the computation of a moving void fraction wave, or in other words to a Riemann problem with well-balanced initial data in the sense defined above, which means that initial left and right states W_L and W_R comply with

$$I^k_{1-2}(W_R) = I^k_{1-2}(W_L) \qquad for: \quad k = 1 - 5.$$

Initial conditions and parameters of EOS for liquid and vapour phases are given in table 3. We recall here that none among existing schemes enables to preserve the exact solution on coarse meshes. Actually, if the initial data W^0_j on the computational domain is such that:

$$I^k_{1,2}(W^0_j) = \mathcal{I}^k_0$$

it may be easily checked that the approximate solutions $I^k_{1,2}(W^1_j)$ at the end of the first time step are not equal to $\mathcal{I}^k_0$, whatever **SR1**, **SR1-ORDER2** or **PFRAC3** is used. Hence, these schemes do not preserve "well-balanced initial data for the VFW". This is roughly the counterpart of the well-known problem of "contact-discontinuity preserving schemes" for Euler equations with complex EOS , and we recall here that some erroneous strategies have been proposed in the literature in order to cope with this problem, since they may enforce convergence towards wrong solutions (see[10]).

Thus we must examine whether the above mentionned schemes enable to recover convergence towards the correct solution when the mesh is refined.

Numerical results that have been computed with first or second-order schemes **SR1**, **SR1-ORDER2** or **PFRAC3** on rather fine meshes are displayed on figures 8 and 10. We have fixed the CFL number to 1/2, and the final time is $t = 0.25$. Meshes contain from 5×10^2 up to 10^5 regular cells. Besides, convergence rates may be obtained using errors provided in figures 7 and 9. We obtain again $h^{1/2}$ and $h^{2/3}$ rates for first and second-order schemes respectively. However, we may note here the rather poor behaviour of the second-order scheme (which of course is not claimed to be the ultimate one). In particular fast left-going and right-going ghost waves are better predicted by the first-order scheme (see figure 10). On the contrary, the void fraction wave is smeared by the second-order scheme, whereas some oscillations arise with the first-order scheme in the same region. On the whole both first and second-order schemes seem to yield similar error levels for a given mesh size, which was actually not expected.

	Exact solution for the void fraction wave VFW		
		Left state(W_L)	Right state(W_R)
GPSG1_A4	α_v	0.05	0.5
	ρ_v	10	12
	u_v	15	15
	p_v	1×10^6	989874.793590249
	ρ_l	1000	999.987662005963
	u_l	10	5.49988278761049
	p_l	1×10^6	967374.092892051
Parameters in PG and SG EOS	$\gamma_v = 1.4$ (Gas) $\gamma_l = 4.4,\ (p_l)_\infty = 6 \times 10^8$(Liquid)		

Table 3. Intial conditions for test case 3 GPSG1_A4 : $(\alpha_v)_L = 0.05$**,** $(\alpha_v)_R = 0.5$

VI. Conclusion

Part of an extensive investigation of some simple first and second-order schemes that may be used to compute approximations of solutions of the Baer-Nunziato model has been reported here; further details and other test cases including various EOS can be found in[28] .

Eventually, we would like to emphasize the following features:

- For all test cases, and whatever the EOS is, we retrieve $h^{1/2}$ and $h^{2/3}$ rates of convergence in L^1 norm, for first and second-order schemes respectively. This was expected (see[10–12] that deal with Euler equations), and it confirms preliminary results of;[23]
- None among existing schemes enables to preserve pure void fraction waves (VFW) on coarse meshes, even when using perfect gas EOS within each phase; nonetheless, basic schemes that have been investigated here yield correct convergence when the mesh is refined; this is in agreement with results of[10] for one-dimensional Euler equations with complex EOS;
- The whole suggests to go further on and benchmark all existing schemes such as those proposed and

described in[1,2,26,33,36] . Moreover, the search for VFW preserving schemes seems to be a challenging and useful purpose for the BN community.

Part of our current work consists in computing water-hammer flow simulations using the present model and numerical techniques.

Acknowledgments:

This work has been achieved in the framework of the EDF R&D SITAR project. Computational facilities were provided by EDF. The last author also receives financial support from ANRT under contract CIFRE 732/2010.

References

[1] Ambroso, A., Chalons, C., Coquel, F., and Galié, T., "Relaxation and numerical approximation of a two-fluid two-pressure diphasic model " *Math. Model. and Numer. Anal.*, vol. 43(6), 2009, pp. 1063–1098.

[2] Ambroso, A., Chalons, C., and Raviart, P.A., "A Godunov-type method for the seven-equation model of compressible two-phase flow " *Computers and Fluids*, vol.54 , 2012, pp. 67-91.

[3] Andrianov, N., and Warnecke, G., "The Riemann problem for the Baer-Nunziato two-phase flow model", *J. Comp. Physics.*, vol. 195, 2004, pp. 434-464.

[4] Baer, M.R., and Nunziato, J.W., "A two-phase mixture theory for the deflagration to detonation transition (DDT) in reactive granular materials", *Int. J. Multiphase Flow*, vol. 12(6), 1986, pp. 861–889.

[5] Baraille, R., "Développement de schémas numériques adaptés à l'hydrodynamique", *PhD thesis*, Université Bordeaux I, Bordeaux, France, 1991.

[6] Bdzil, J.B., Menikoff, R., Son, S.F., Kapila, A.K., and Stewart D.S., "Two-phase modeling of a DDT in granular materials: a critical examination of modeling issues", *Phys. of Fluids*, vol. 11, 1999, pp. 378-402.

[7] Chalons, C., Coquel, F., Kokh, S., and Spillane, N. "A relaxation method to compute approximations of the Baer-Nunziato model" *Proceedings of Finite Volumes for Complex Applications VI*, Fort, Fürst, Halama, Herbin, Hubert editors, Springer-Verlag, 2011, pp. 225-234.

[8] Coquel, F., Gallouët, T., Hérard, J.M., and Seguin, N., "Closure laws for a two-fluid two-pressure model", *C. R. Acad. Sci. Paris*, vol. I-332, 2002, pp. 927–932.

[9] Gallouët, T., Helluy, P., Hérard, J.-M., and Nussbaum, J., "Hyperbolic relaxation models for granular flows", *Math. Model. and Numer. Anal.*, vol.44(2), 2010, pp.371-400.

[10] Gallouët, T., Hérard, J.-M., and Seguin, N., "A hybrid scheme to compute contact discontinuities in one-dimensional Euler systems", *Math. Model. and Numer Anal.*, vol. 36(6), 2002, pp. 1133-1159.

[11] Gallouët, T., Hérard, J.-M., and Seguin, N., "Some recent Finite Volume schemes to compute Euler equations using real gas EOS", *Int. J. Num. Meth. Fluids*, vol. 39(126), 2002, pp. 1073-1138.

[12] Gallouët, T., Hérard, J.-M., and Seguin, N., "On the use of symmetrizing variables for vacuum", *Calcolo*, vol. 40 (3), 2003, pp. 163-194.

[13] Gallouët, T., Hérard, J.-M., and Seguin, N., "Numerical modelling of two phase flows using the two-fluid two-pressure approach", *Math. Mod. Meth. in Appl. Sci.*, vol. 14(5), 2004, pp. 663-700.

[14] Gavrilyuk, S., and Saurel, R., "Mathematical and numerical modelling of two phase compressible flows with inertia", *J. Comp. Physics.*, vol. 175, 2002, pp. 326-360.

[15] Girault, L., and Hérard, J.-M., "A two-fluid hyperbolic model in a porous medium", *Math. Model. and Numer. Anal.*, vol. 44(6), 2010, pp. 1319-1348.

[16] Girault, L., and Hérard, J.-M., "Multidimensional computations of a two-fluid hyperbolic model in a porous medium", *Int. J. Finite Volumes*, URL: http://www.latp.univ-mrs.fr/IJFV/, vol. 7(1), 2010, pp. 1-33.

[17] Godunov, S.K., "Finite difference method for numerical computation of discontinuous solutions of the equations of fluid dynamics", *Mat. Sb.*, vol. 47, 1959, pp. 271-300.

[18] Guillemaud, V., "Modélisation et simulation numérique d'écoulements diphasiques par une approche bifluide à deux pressions", *PhD thesis*, Université Aix-Marseille I, Marseille, France, 2007.

[19] Hérard, J.-M., "A three-phase flow model", *Mathematical Computer Modelling*, vol. 45, 2007, pp. 432-455.

[20] Hérard, J.-M., "An hyperbolic two-fluid model in a porous medium", *Comptes-rendus Mécanique*, vol. 336, 2008, pp. 650-655.

[21] Hérard, J.-M., "Une classe de modèles diphasiques bi-fluides avec changement de régime", *internal EDF report H-I81-2010-0486-FR, in French*, unpublished, 2011.

[22] Hérard, J.-M., and Hurisse, O., "Schémas d'intégration du terme source de relaxation des pressions phasiques pour un modèle bifluide hyperbolique", *internal EDF report H-I81-2009-1514-FR, in French*, unpublished, 2009.

[23] Hérard, J.-M., and Hurisse, O., " A fractional step method to compute a class of compressible gas-liquid flows", *Computers and Fluids*, vol.55 , 2012, pp. 57-69.

[24] Kapila, A.K., Menikoff, R., Bdzil, J.B., Son, S.F., and Stewart, D.S., "Two-phase modeling of a DDT in granular materials: reduced equations", *Phys. of Fluids*, vol. 13, 2001, pp. 3002-3024.

[25] Kapila, A.K., Son, S.F., Bdzil, J.B., Menikoff, R., and Stewart, D.S., "Two-phase modeling of a DDT: structure of the velocity relaxation zone", *Phys. of Fluids*, vol. 9(12), 1997, pp. 3885–3897.

[26] Karni, S., and Hernandez-Duenas, G., "A hybrid algorithm for the Baer Nunziato model using the Riemann invariants", *SIAM J. of Sci. Comput.*, vol.45, 2010, pp.382-403.

[27] Kroner, D., and Thanh, M.D., "Numerical solution to compressible flows in a nozzle with variable cross-section", *SIAM J. of Num. Anal.*, vol.43, 2006, pp.796-824.

[28] Liu, Y., PhD thesis, Université Aix Marseille I, Marseille, France, *in preparation*, 2013.

[29] Lowe, C.A., " Two-phase shock-tube problems and numerical methods of solution", *J. Comp. Physics.*, vol. 204, 2005, pp. 598-632.

[30] Ransom, V., and Hicks, D.L., "Hyperbolic two-pressure models for two-phase flow", *J. Comp. Physics.*, vol. 53, 1984, pp. 124-151.

[31] Rusanov, V., "Calculations of interaction of non-steady shock waves with obstacles", *Computational Mathematics and Mathematical Physics*, vol. 1, 1961, pp. 267-279.

[32] Saleh, K., PhD thesis, Université Pierre et Marie Curie, Paris, France, *in preparation*, 2012.

[33] Schwendeman, D.W., Wahle, C.W., and Kapila, A.K., " The Riemann problem and a high-resolution Godunov method for a model of compressible two-phase flow ", *J. Comp. Physics.*, vol. 212, 2006, pp. 490-526.

[34] Thanh, M.D., "The Riemann problem for a non-isentropic fluid in a nozzle with discontinuous cross-sectional area", *SIAM J. of Appl. Math.*, vol.69 (6), 2009, pp.1501-1519.

[35] Giot, M., Prasser, H.M., Dudlik, M., Ezsol, G., Habip, M., Lemonnier, H., Tiselj, I., Castrillo, F., Van Hove, W., Perezagua, R., and Potapov, S, "Two-Phase Flow Water Hammer Transients and Induced Loads on Materials and Structures of Nuclear Power Plants (WAHALoads)", *contract FIKS-CT-2000-00106*, 2000.

[36] Tokareva, S.A., and Toro, E.F., " HLLC type Riemann solver for the Baer-Nunziato equations of compressible two-phase flow", *J. Comp. Physics.*, vol. 229, 2010, pp. 3573-3604.

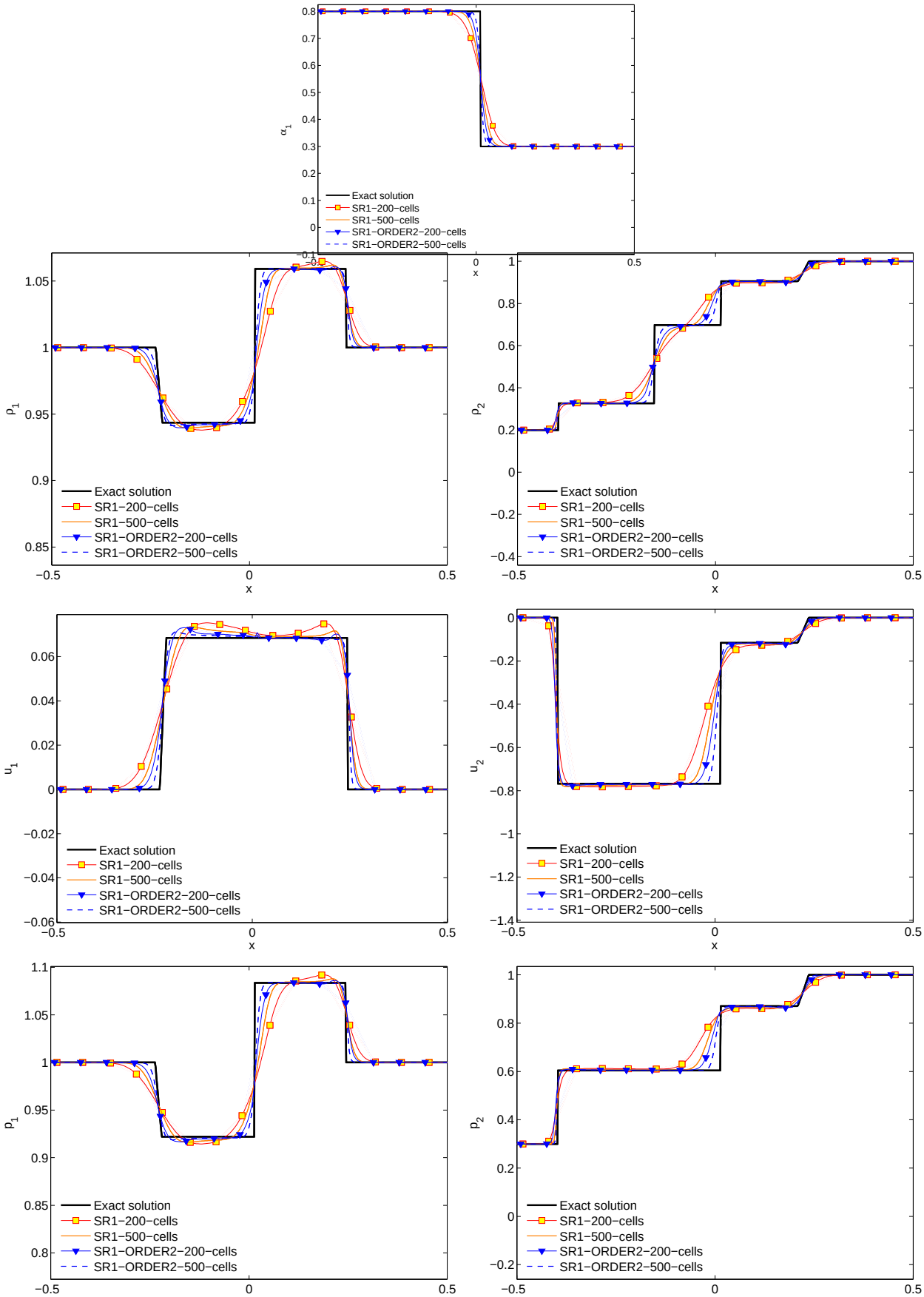

Figure 2. Approximate solutions for variables $\alpha_1, \rho_k, u_k, p_k, k = 1, 2$ for test case 1 by Schwendeman-Wahle-Kapila, with first-order and second-order Rusanov schemes (SR1 and SR1-ORDER2), using meshes with 200 and 500 cells, setting $CFL = 0.5,\ t = 0.2$.

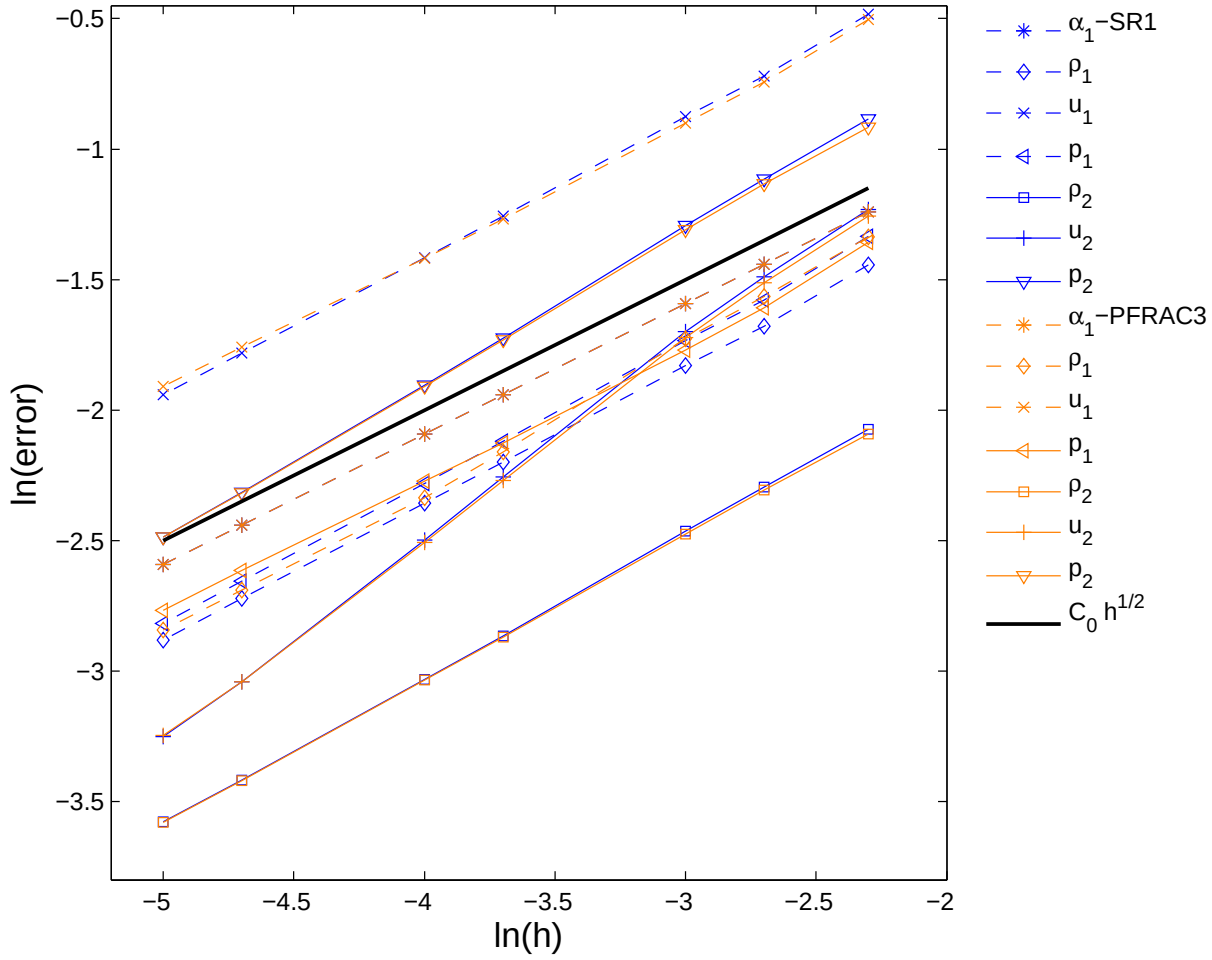

Figure 3. L^1 **norm of the error for variables** $\alpha_1, \rho_k, u_k, p_k,\ k = 1, 2$ **for test case 2 with SR1, PFRAC32 with** $CFL = 1/2,\ t = 0.15$

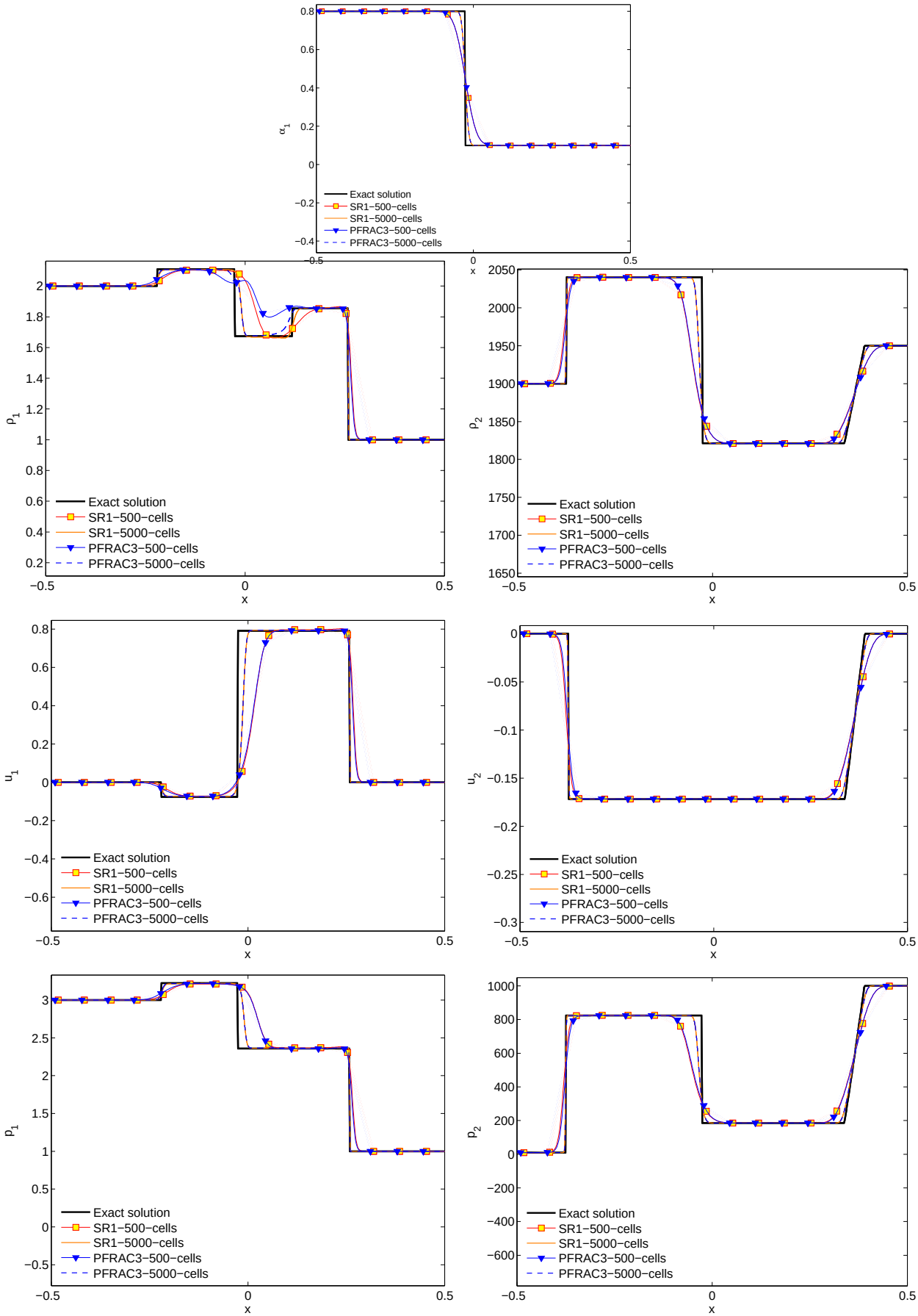

Figure 4. Approximate solutions for variables $\alpha_v, \rho_k, u_k, p_k, k = l, v$ for test case 2 by Tokareva and Toro , using SR1, and PFRAC32 schemes with 500 and 5000 cells. $CFL = 1/2,\ t = 0.15$

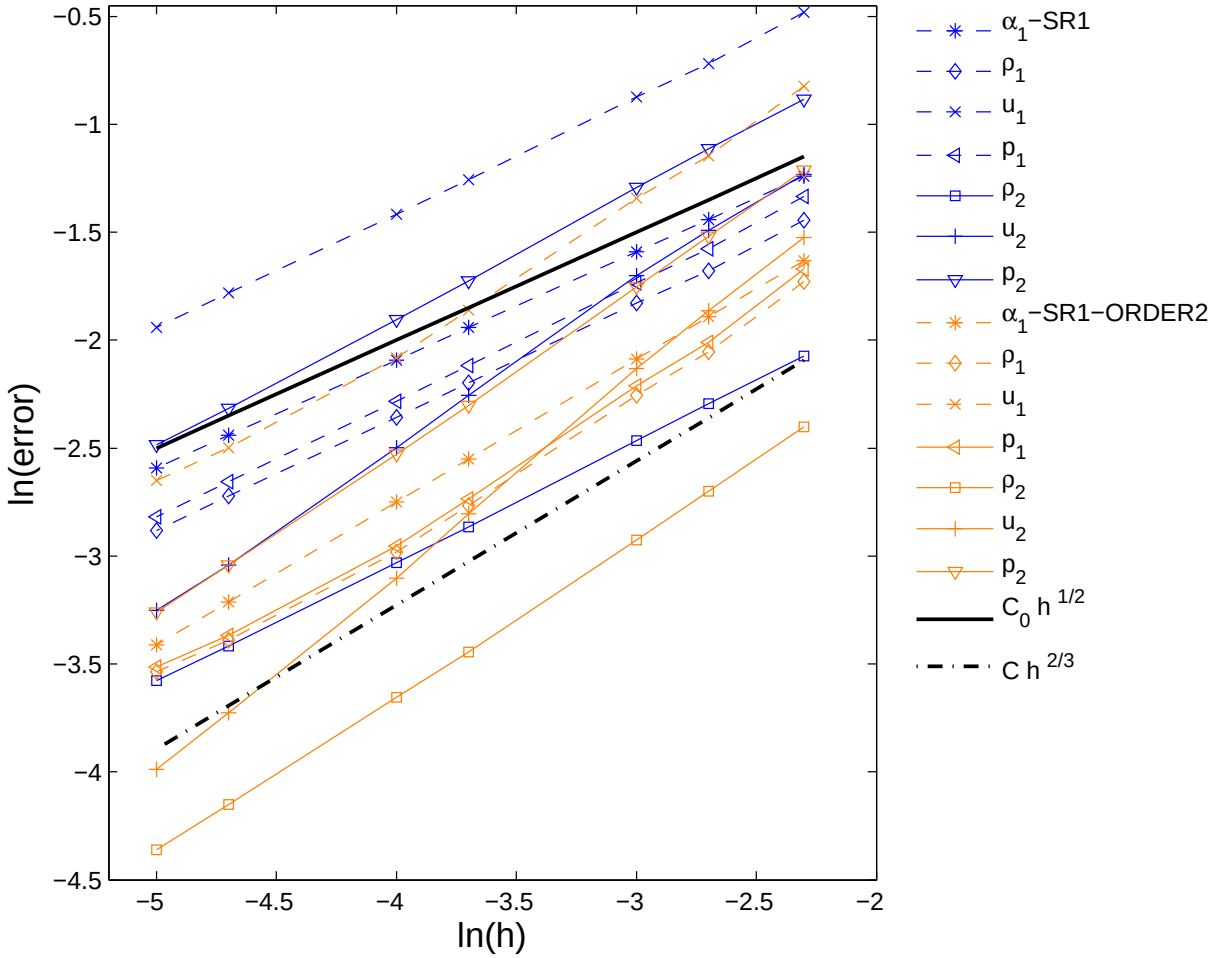

Figure 5. L^1 **norm of the error for variables** $\alpha_v, \rho_k, u_k, p_k,\ k = l, v$ **for test case 2 by Tokareva and Toro, with schemes SR1 and SR1-ORDER2, setting:** $CFL = 1/2,\ t = 0.15$

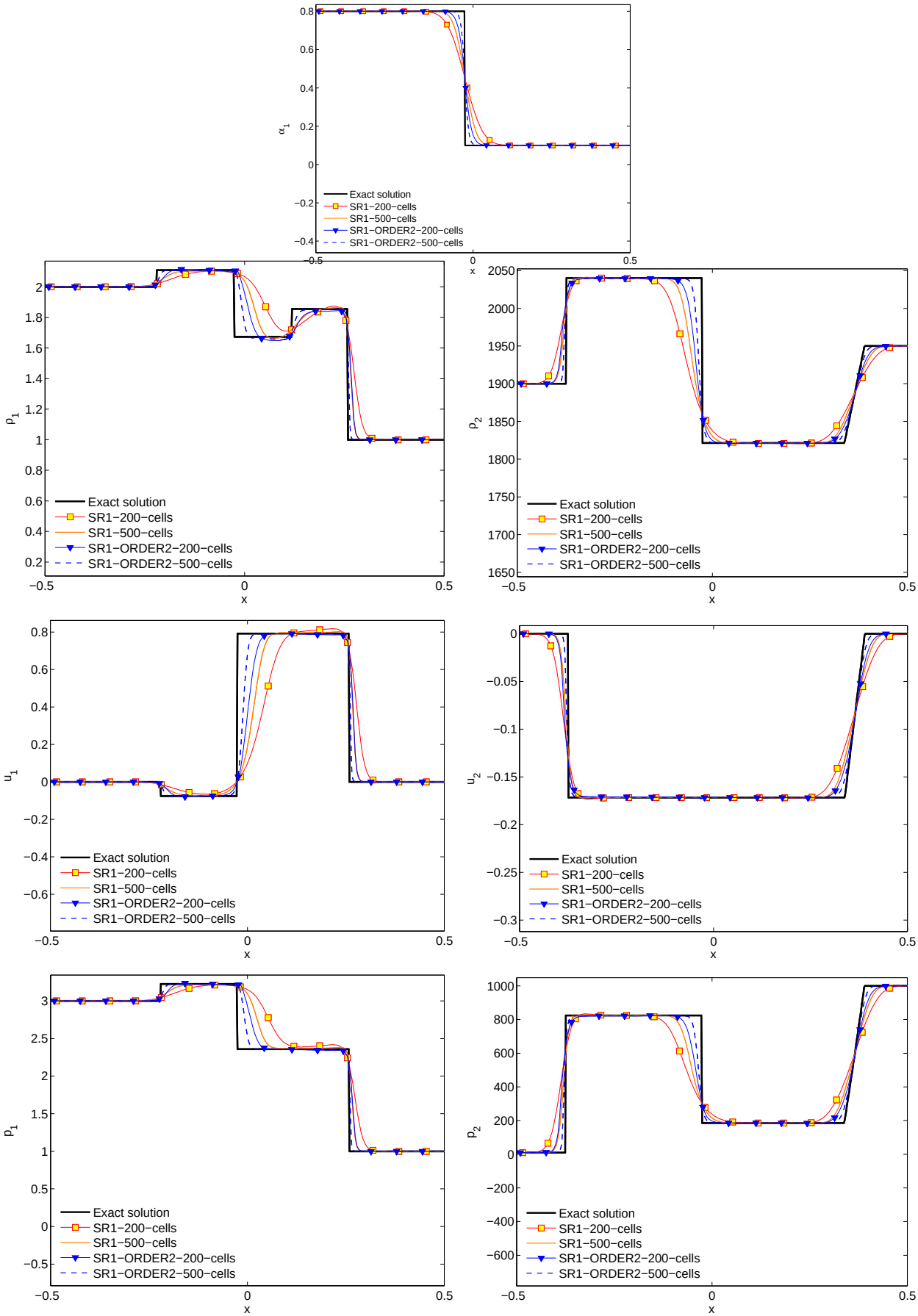

Figure 6. Approximate solutions for variables $\alpha_v, \rho_k, u_k, p_k, k = l, v$ for test case 2 by Tokareva and Toro, for first and second-order schemes SR1, SR1-ORDER2, with 200, 500 cells, setting $CFL = 1/2,\ t = 0.15$

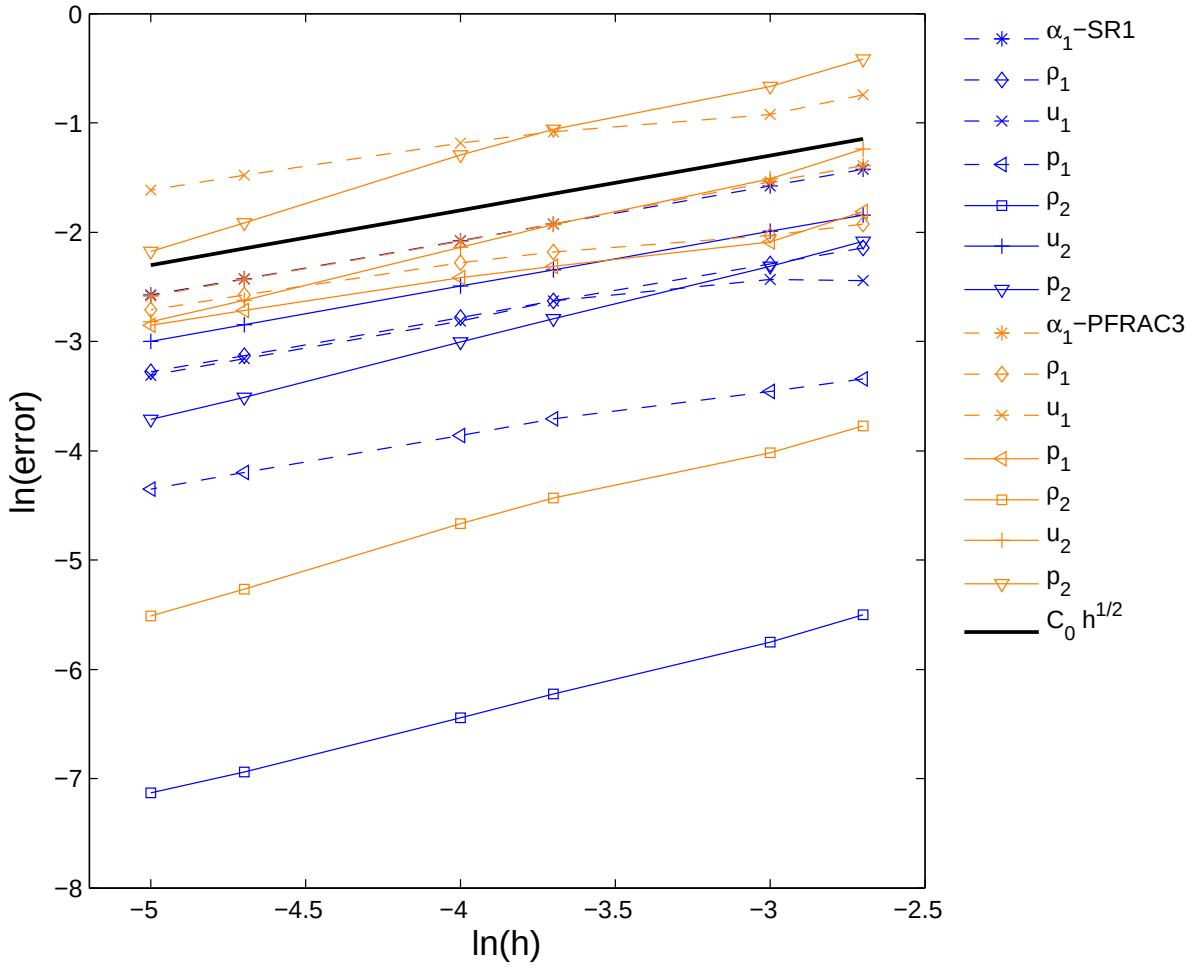

Figure 7. L^1 **norm of the error for variables** $\alpha_v, \rho_k, u_k, p_k$, $k = l, v$ **for test case 3 of a moving VFW, with schemes SR1 and PFRAC**3 ($CFL = 1/2$, $t = 0.25$)**.**

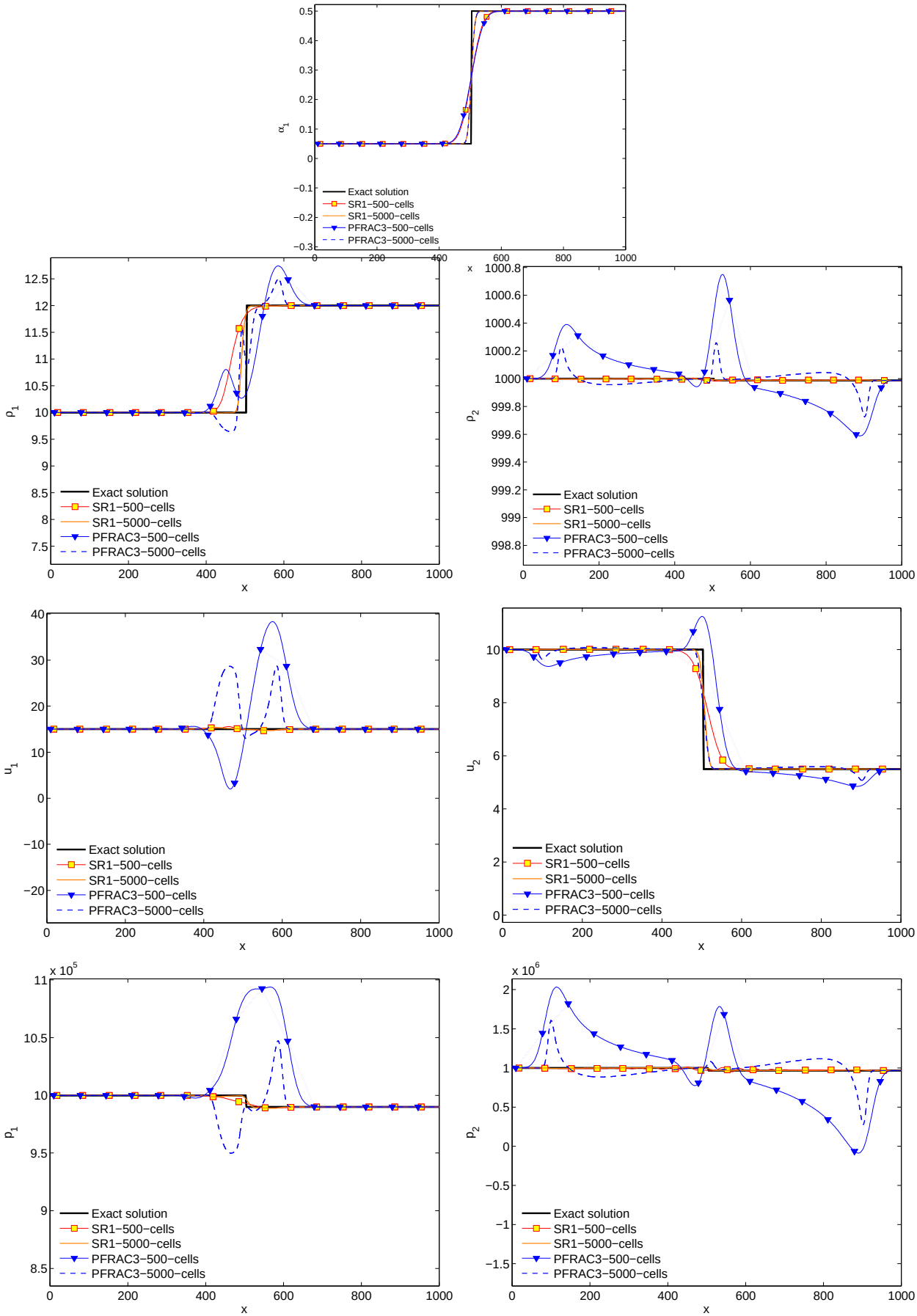

Figure 8. Approximate solutions for variables $\alpha_1, \rho_k, u_k, p_k, k = 1, 2$ for test case 3 of a moving VFW, with first-order Rusanov schemes SR1, PFRAC3, using 500 and 5000 cells ($CFL = 1/2,\ t = 0.25$).

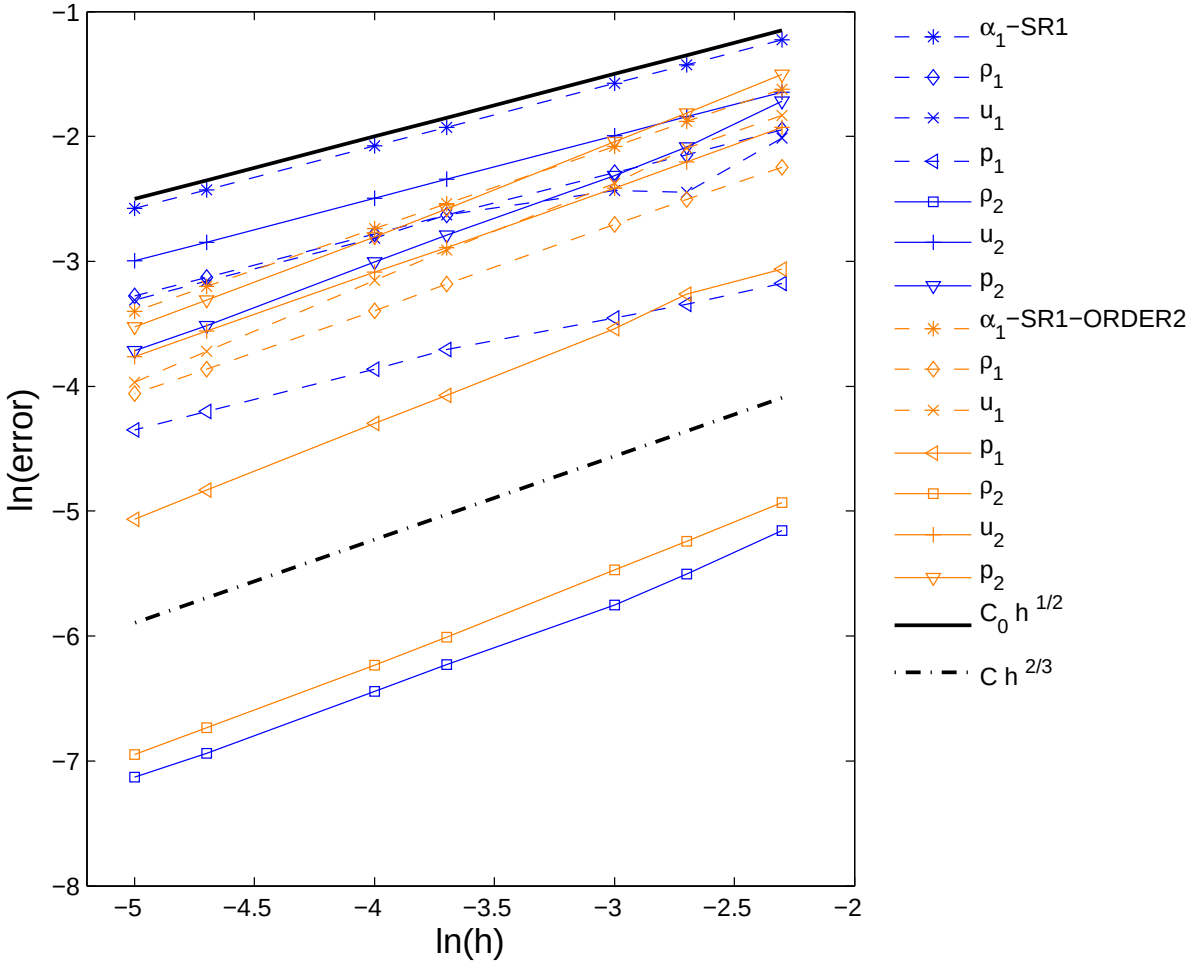

Figure 9. L^1 **norm of the error for variables** $\alpha_v, \rho_k, u_k, p_k$, $k = l, v$ **for test case 3 of a moving VFW, with schemes SR1 and SR1-ORDER2** ($CFL = 1/2$, $t = 0.25$)**.**

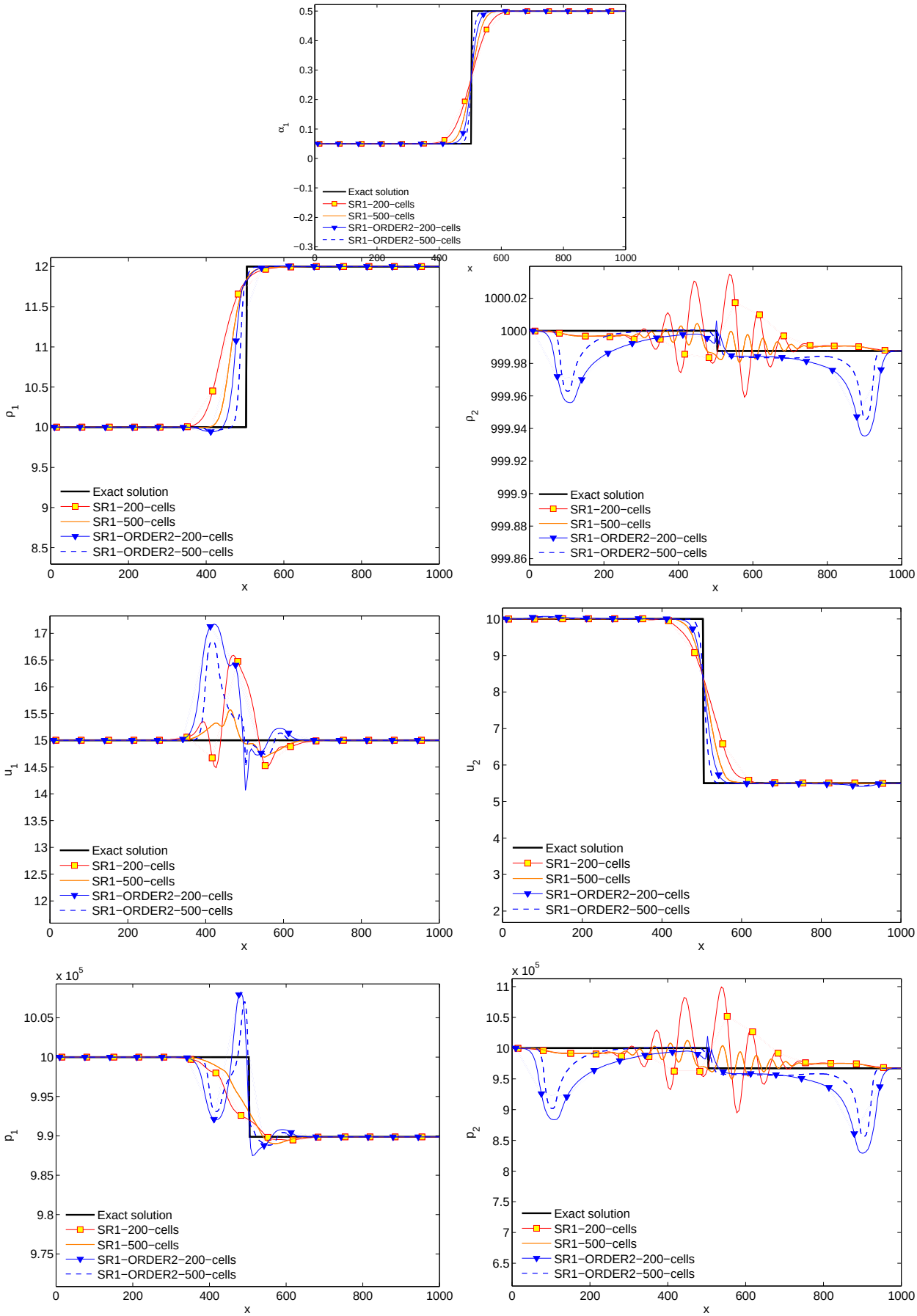

Figure 10. Approximate solutions for variables $\alpha_v, \rho_k, u_k, p_k, k = l, v$ for test case 3 of a moving VFW, using first and second-order schemes SR1, SR1-ORDER2 with meshes containing 200 and 500 cells ($CFL = 1/2,\ t = 0.25$)